ELSEVIER

Catalysis Today 53 (1999) 145–158

CATALYSIS TODAY

www.elsevier.com/locate/cattod

Aerobic and anaerobic TiO_2-photocatalysed purifications of waters containing organic pollutants

Joseph Cunningham *, Ghassan Al-Sayyed, Petr. Sedlak, John Caffrey

Chemistry Department, University College Cork, Cork, Ireland

Abstract

Developments reported by European research groups in removal of dilute organic pollutants from water under the combined action of TiO_2 particles and solar-illumination are briefly outlined. Instances are given of poor correlation between trends actually observed for selected TiO_2*-photocatalysed conversion in aerobic conditions and trends expected within the context of two-parameter Langmuir–Hinshelwood-type rate expressions. The necessity of recognising important kinetic roles of several parameters is emphasised not only for aerobic, but also for anaerobic conditions, e.g. TiO_2*-photocatalysed conversions of chloromethane pollutants in deoxygenated aqueous solutions. Comparisons between initial TiO_2-sensitized photocatalytic degradation (TiO_2*-PCD) rates versus dark-equilibrated $[C]_{eq}$ profiles for one *strongly-adsorbed* and one *weakly-adsorbed* pollutant in aerated TiO_2 suspensions at concentrations <100 ppm imply that, under high photon flux, the former can be more strongly inhibited in consequence of: (i) chemisorption-induced depletions of surface OH^- groups; (ii) adsorbate-enhanced hole–electron recombinations on the TiO_2* surfaces (iii) mass transport limitations within the TiO_2 particle aggregates. Insights into the nature of strongly chemisorbing pollutants (e.g. hydroxybenzoic acids or catechol) onto TiO_2(P25) were obtained by DRIFTS measurements upon freeze-dried TiO_2 powder samples after their dark-equilibration with 3–100 ppm solutions.

Keywords: TiO_2 photocatalysis; Adsorption isotherm; Chelated adsorbate; DRIFTS spectra; Monochlorophenols; Hydroxybenzoic acid

1. Introduction

Upon receiving the invitation to present a paper on the above topic at this European Research Conference I felt it would be appropriate to commence with brief accounts of important recent progress achieved by other European groups in applying TiO_2-sensitized photocatalytic degradation (TiO_2*-PCD) of various organic contaminants in polluted waters [1–11]. Hopefully, this introduction will serve *not only* to indicate the wide range of organic pollutants whose removal from waters can now be effected thanks to innovative developments in photocatalytic reactor design and in the utilization of solar illumination, *but also* to indicate where needs exist for significant revision of some frequently utilised mechanistic ideas concerning TiO_2*-PCD. Subsequent parts of the paper will outline results from research at University College Cork which has been vectored towards identifications of the several parameters which affect TiO_2*-PCD rates and efficiencies. Implications of the results in respect of improved mechanistic ideas are also considered.

An outline representation is given in Scheme 1 of how absorption of UV-photons ($\lambda \leq 390$ nm) may result, via TiO_2* exciton formation (not shown), in separation of some excitons into e^-/S_e, a conduction-band electron localised upon S_e, an electron-trapping

* Corresponding author. +353-21-902454; fax: +353-21-274097
E-mail address: stch8058@bureau.ucc.ie (J. Cunningham)

0920-5861/99/$ – see front matter
PII: S0920-5861(99)00109-1

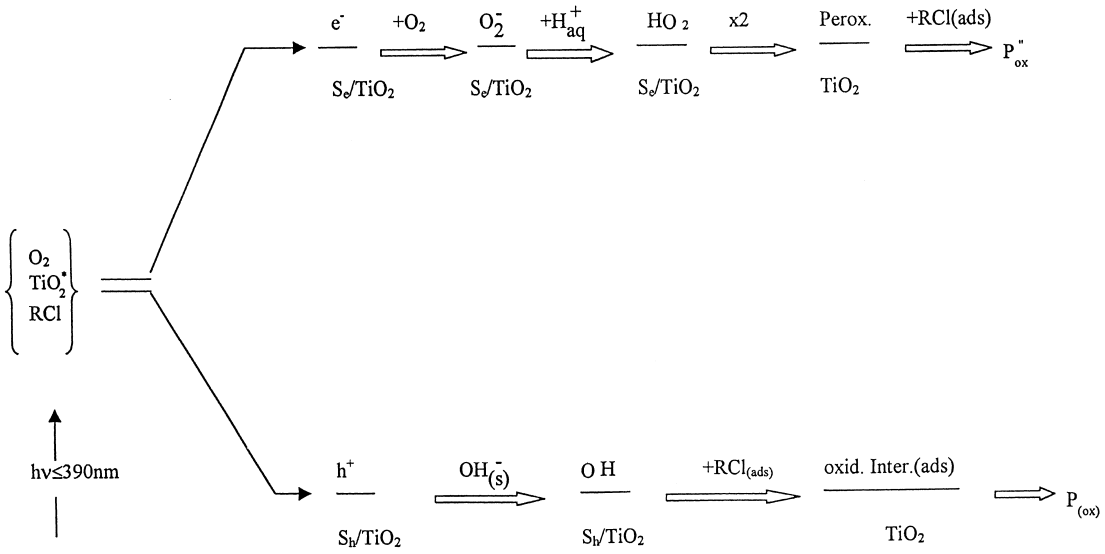

Scheme 1. Outline of the reaction sequences initiated by near-UV illumination producing photogenerated electrons (reactions as per upper branch) and photogenerated holes (reactions as per lower branch) originated at surfaces of TiO_2 particles/aggregates suspended in aerated aqueous solutions containing pollutant RCl.

surface site or species, *plus* h^+/S_h a valence band hole localised upon S_h, a hole-trapping surface site or species. The low efficiency of such localization processes relative to fast recombination of non-trapped or partially trapped TiO_2*excitons, is mainly responsible for the low photonic efficiencies normally obtained in TiO_2 sensitized PCD.

The sequence of post-primary events represented on the upper branch of Scheme 1 as originating from e^-/S_e typify those usually considered to occur at microinterfaces between photoactivated TiO_2^* particles and aerated or oxygenated aqueous solutions: viz. electron-capture by O_2 at the interface, conversion of O_2^- to HO_2, and oxidative attack by the latter upon pollutant species. Gerischer and Heller have expressed the view [3] that this electron-trapping role of O_2 can be the rate- and efficiency-determining-process, and many investigators have demonstrated that rigorous deoxygenation of aqueous solution/TiO_2^*-suspensions results in complete loss of capability of many systems for TiO_2*-PCD (but see later for a notable exception).

The lower branch of Scheme 1 represents one version of the sequence of oxidative events initiated by those h^+/S_h locations which, aided by the electron-trapping role of O_2, escape recombination with e^-/S_e, viz. rapid transfer of h^+/S_e to one OH^- group within the well-hydroxylated TiO_2 surface layer, yielding an OH radical which oxidatively attacks pollutant molecules at or close to that layer. That simplified representation will not provide a fully adequate representation of the sequence of oxidative events in cases where direct transfer of h^+/S_h to pollutant molecules adsorbed within the hydrated surface layer serve as an additional alternative primary step towards oxidised product [4,5]. In his studies of one such system Richard determined the relative extents to which three possible oxidative products from 4-hydroxy benzyl-alcohol HBA, – two attributable to OH-radical attack and one to h^+ attack – were produced by TiO_2*-PCD versus their production by Fenton's reagent [5]. He concluded that positive holes and hydroxyl radicals had different regioselectivities in TiO_2*-PCD of HBA, hydroquinone being produced by h^+-attack, dihydroxybenzyl alcohol by OH attack and 4-hydroxy benzaldehyde via attacks by both h^+ and OH.

In respect of oxidative degradations of a wide range of organic pollutants in aerated waters, much valuable technical progress has been achieved using solar illumination to drive TiO_2*-PCD within the context of Scheme 1. Information on several of those processes have been provided by Dr. Blanco in his lead-in

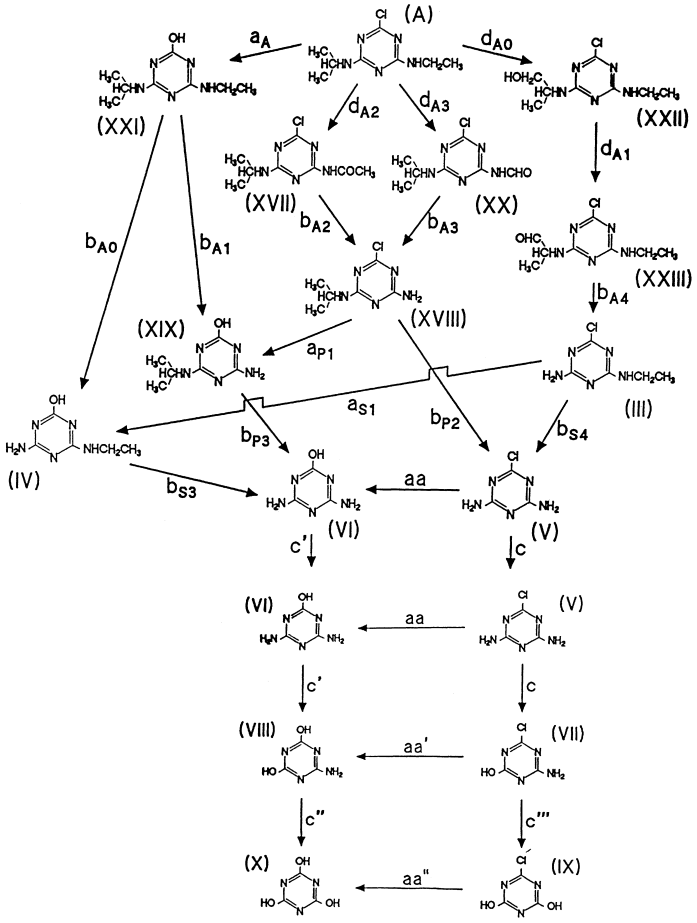

Scheme 2. Complex network of TiO_2*-photogenerated primary transformations of atrazine (A) in aerated aqueous suspensions, showing also the identities of intermediates formed initially and during their transformations ultimately to non-toxic cyanuric acid (X) [8].

presentation to session – and by various workers in several posters at this meeting. Consequently I shall concentrate on just a few examples, which not only typify the impressive progress achieved but can also serve to illustrate the need for improved understanding of the basic processes involved. My first pair of examples relate to solar-illumination induced TiO_2*-PCD of the herbicide atrazine and the wood-preservative pentachlorophenol [6,7]. Run-off from uses of those and structurally-related toxic materials have, in some areas, resulted in their build-up to unacceptable levels in the water table. Removal of toxic atrazine from such waters was effected by TiO_2*-PCD, whereby atrazine was converted to non-toxic cyanuric acid in accordance with the following equation: $C_8H_{14}ClN_5 + 15/2\ O_2 \rightarrow C_3N_3(OH)_3 + 5CO_2 + 5H_2O$ [6]. A large solar plant photocatalytic system was used featuring one Helioman unit through whose illuminated phototubes a suspension containing 200 mg TiO_2 l^{-1} was recirculated at 4000 l h^{-1} under near-UV-intensity equivalent to six suns [6]. The on-site confirmation of success in thus decreasing atrazine concentration to levels well below limits specified in EC legislation, albeit with just 2% efficiency of absorbed near-UV-photons in effecting removal of the lateral alkyl side chains, had been preceded by very detailed chemical analyses to identify whatever intermediates developed from UV-illumination of aerated $(Atrazine)_{aq}/TiO_{(P25)}$ suspensions at various stages [8]. Such information was then used to develop Scheme 2 as a representation of

the complex network of individual reactions via which TiO_2*-PCD of atrazine to cyanuric acid proceeded. An important benefit from establishment of that complex network, on the basis of detailed chemical analyses, was the reassurances it provided in respect of non-persistence of intermediates (non-toxic or otherwise) by virtue of their rapid consumption en-route to non-toxic cyanuric acid as sole product. On the other hand, the possibility seemed remote that kinetics of TiO_2*-PCD of atrazine (AZ) proceeding via such a complex network of reactions could receive a physically meaningful representation on the basis of a two-parameter equation such as

$$-\frac{d[C_{AZ}]}{dt^*} = k_{LH}\frac{K_{AZ}C_{eq}}{1 + K_{AZ}C_{eq}} \quad (1)$$

A common interpretation of the two parameters K_{AZ} and k_{LH} in such a Langmuir–Hinshelwood-type rate-expression would be that they correspond respectively to (i) an equilibrium constant for adsorption–desorption of atrazine between its aqueous solution and the TiO_2 surface, and (ii) a specific rate-constant for reaction between adsorbed atrazine and sites/species upon TiO_2 activated as per the lower half of Scheme 1.

The low probability that just two such parameters, having the indicated physical signficances, could be the only factors controlling TiO_2*-PCD processes involving complex reaction networks similar to that illustrated in Scheme 2 was critically examined by Minero et al [9] in respect of solar illumination-induced TiO_2*-PCD of pentachlorophenol PCP. In one strand of their critical analysis they compared parameters obtained from double-reciprocal plots of (extent of PCP adsorption)$^{-1}$ versus $[PCP]_{eq}{}^{-1}$ and of (initial TiO_2*-PCD rate)$^{-1}$ versus (initial [PCP])$^{-1}$ to deduce experimentally-based values for K_{eq} and k_{LH}. The second strand in their approach involved modelling the kinetics expected on the basis of TiO_2*-PCD proceeding via a reaction network of intermediate reactions of comparable complexity to Scheme 2. From this double-stranded approach they concluded that "whilst experimental data can be fit by an approximate kinetic solution which has the analytical form of a Langmuir-Hinshelwood equation, nevertheless the parameters of such working model equation have been demonstrated not to have physical significance". Minero arrived at a similar conclusion from detailed kinetic analysis of another TiO_2*-PCD process [10]. A healthy scepticism is thus appropriate in respect of values of k_{LH} and K_{ads} parameters deduced solely on the basis of L–H-based, double-reciprocal-type plots of (rates of aqueous pollutant removal by TiO_2*-PCD)$^{-1}$ versus (aqueous pollutant concentration)$^{-1}$.

Recent advances in two qualitatively different utilizations of TiO_2*-PCD for water-depollution also merit mention in this section, namely: (a) demonstrations that chloromethanes can successfully be degraded by UV-illumination of oxygen-free aqueous solutions having TiO_2 suspended therein, and (b) photoactivation of TiO_2 immobilized upon various supports in contact with aerated/oxygenated aqueous solutions which contain pollutants.

(a) Indications that TiO_2*-PCD of waters polluted by chloromethanes can proceed by photoactivated processes additional to those represented in Scheme 1 follow from recent reports by Calza et al. of their success in achieving TiO_2*-PCD of chloromethanes in *deoxygenated* aqueous suspensions [11,12]. Stoichiometry of those processes has been represented by the following Eqs. (2)

$$CCl_4(aq) + 2H_2O(l) \rightarrow CO_2(g) + 4HCl(aq) \quad (2A)$$

$$CHCl_3(aq) + 2H_2O(l) \rightarrow HCOOH(aq) + 3HCl(aq) \quad (2B)$$

$$CH_2Cl_2(aq) + H_2O(l) \rightarrow HCHO + 2HCl \quad (2C)$$

$$2CH_2Cl_2(aq) + 3H_2O(l) \rightarrow HCOOH(aq) + CH_3OH(aq) + 4HCl(aq) \quad (2D)$$

The fact that carbon has +4 oxidation number on both sides of Eq. (2)(A) points to one major mechanistic difference between that anaerobic TiO_2*-PCD process and others proceeding by redox reactions in aerated suspensions in accordance with Scheme 1, since those latter usually resulted in increase of the oxidation number of carbon to +4. Pellizzetti and co-workers therefore referred to the conversions in Eq. (2)(A–D) being formally hydrolyses or disproportionations. Another difference from Scheme 1, which could be implied from the observed occurrence of the above equations in the absence of O_2,

was that the electron-trapping role assigned to O_2 in the former is replaced by electron-trapping roles of the chloromethanes. For example, the initial processes proposed in TiO_2*-PCD of CCl_4 included the following:

$$CCl_4 + e^- \rightarrow CCl_3 + Cl^- \quad (3A)$$

$$CCl_4 + 2e^- \rightarrow CCl_3^- + Cl^- \quad (3B)$$

$$CCl_4 + 2e^- + H^+ \rightarrow CHCl_3 + Cl^- \quad (3C)$$

Painstaking chemical analyses of all species present in illuminated oxygen-free suspensions after various periods of illumination resulted in identifications of all intermediates and made possible time-profiles for their production and eventual disappearance during the TiO_2*-PCD of CCl_4, $CHCl_3$ and CH_2Cl_2 [11]. Calza et al. thus developed a complex network of reaction events – including attack by OH, and substitution reactions e^-/–Cl^- and OH^-/–Cl^- and H_2O/–HCl; plus the corresponding reverse processes – with which to account for the intermediates observed and pathways followed en-route to the product stoichiometries indicated in Eq. (2)(A–D).

(b) An important practical advantage sought through the use of immobilised TiO_2 as the photoinitiator in TiO_2*-PCD, as distinct from TiO_2 particles suspended in a polluted aqueous phase, is avoidance of the need for filtration to remove the suspended TiO_2 particles before return of the depolluted water to desired re-use. Progress via Scheme 1 should apply, provided that the aqueous phase circulating over the immobilised TiO_2 is oxygenated or aerated. Full accounts have been given by Bauer at this conference of wide-ranging success in depollution of variously contaminated waters by flowing them over a specially designed photoreactor featuring TiO_2 immobilised upon surfaces of a large bundle of thin cylindrical quartz supports. Efficiency of delivery/penetration of the UV-illumination to TiO_2 thus immobilized is enhanced relative to its poorer penetration into aqueous suspensions containing TiO_2 particles.

Other recent applications of immobilised TiO_2 layers have involved their deposition onto flat surfaces which are both transparent and electrically conducting, thereby allowing the combination to serve as an optically transparent electrode (OTE). [13–15]. Under UV-illumination from the non-TiO_2-coated side, whilst a suitable positive bias is applied, the OTE tends to withdraw some electrons from the UV-illuminated TiO_2 layer thereby substituting for the electron-trapping role of O_2 (cf. Scheme 1), and allowing studies of TiO_2*-PCD related processes in deoxygenated solutions. Conversely TiO_2*-photogenerated holes experience repulsion towards the TiO_2//aqueous-solution interface and can enhance oxidative degradation in deoxygenated systems [13,14]. Tada et al. have explored the relationship between thickness of the TiO_2 layer immobilised upon the OTE and the effectiveness of reverse-side illumination in causing a measurable physical change at the outermost surface of the layer [15]. Maximum effectiveness occurred for layer thickness ca. 100 nm, above which it decreased. They attributed such decrease to increased percentage loss of photoinduced e^- and h^+ by virtue of increased recombinations within greater layer thicknesses. They argued that a value of $2 \times 10^{-2}\,cm^2\,s^{-1}$ estimated from their results for diffusion of primary photogenerated charge carriers were in fairly good agreement with corresponding literature values and consistent with lifetimes $\tau \sim 100$ ns [16].

2. Experimental

2.1. Materials

The titanium powder used for measurements was Degussa TiO_2(P25) powder specified as having 80/20 anatase/rutile composition, primary particle size ~30 nm and BET surface area $50\,m^2\,g^{-1}$. Surface impurities were removed by overnight preoxidation under a flow of high-purity, dried O_2 at 823 K prior to measurements of the adsorption or photocatalytic properties at 295 K. HPLC-grade water was used in preparation of all solutions. Hydroxybenzoic acids (HBA) or phenols (PhOH) were the highest purity available from Aldrich.

2.2. Concentration dependence of equilibrium extents of adsorption at 295 K

Following introduction of 200 mg of precalcined TiO_2 plus 100 ml of $(HBA)_{aq}$ or $(PhOH)_{aq}$

into stoppered and blackened Erhlenmeyer flasks, these were shaken overnight to ensure attainment of equilibrium-dark adsorption. The unadjusted pH of the suspensions evidenced pH values of 5.5 ± 0.5. A (TiO_2 + water) reference was likewise dark-equilibrated. Filtration through Millipore 0.4 or 0.2 μ membrane filters next morning was used to separate the adsorption dark-equilibrated solutions from the TiO_2 powder. Concentrations of HBA or PhOH in the filtrates were determined by HPLC. Values for the amount removed from solution by virtue of equilibrium extent of adsorption were then deduced from concentration decrease relative to an aliquot of solution not contacted with TiO_2. They are expressed as $n^s{}_2$, μmol adsorbed per gram of TiO_2.

DRIFTS measurements upon aliquots of TiO_2 powder separated by filtration (as above) from their equilibrium-dark-equilibrated solutions were performed after the following work-up: TiO_2 powder retained by the Millipore filter was freeze-dried under continuous pumping overnight at -40^oC; then it was permitted to warm-up to 295 K within its evacuated freeze-drying container before transfer into the sample holder of a diffuse reflectance accessory (PEDR) and measurement on an FTIR Spectrometer (Perkin–Elmer Paragon 1000). An identical set of steps was applied to TiO_2 which had been equilibrated with pure water. Difference-spectra (in Kubelka-Munk form) between that of the TiO_2 reference and those from TiO_2 samples which had been dark-equilibrated with a solution having HBA or PhOH concentrations 3, 10, 30 or 100 ppm were obtained and compared.

2.3. Concentration and intensity dependence of $TiO_2{}^*$-photoinitiated rates of decrease in $[HBA]_{aq}$ and $[PhOH]_{aq}$ from C_{eq} their dark-equilibrated concentrations

Dark pre-equilibration was first established between 30 ml of solution and 60 mg of precalcined TiO_2 powder in a stirred photoreactor. After flushing with pure O_2 or purified air, this was sealed. Provision was made for later syringe-extraction of small aliquots of the stirred suspension via rubber septa sealed side arms. After ≥1 h pre-equilibration of the stirred suspension in the dark, illumination commenced with photons having $\lambda| = 365 \pm 10$ nm (selected by interposing the appropriate narrow-band-pass filter between the transparent bottom window of the photoreactor and a 125 W medium-pressure Hg lamp). This yielded a flux of 2×10^{18} photons min^{-1} incident into the photoreactor volume. When so desired a *medium* flux of 5.6×10^{17} photons min^{-1} or a *low* flux of $1.7 \times 10^{16}\,min^{-1}$ (as determined using chemical actinometer solutions) were obtained by interposing metal gauze screens in the light path. After various durations of illumination, samples of the continuously stirred and illuminated suspension were syringe-extracted, filtered through 0.2 μm membranes and the clear filtrate analysed by HPLC. Concentrations thus determined were plotted versus duration of UV-illumination.

3. Results and interpretation

3.1. Substantial qualitative difference between 'dark' adsorption isotherms of 3-chloro-4-hydroxybenzoic acid (CHBA) and monochlorophenols (ClPhOH)

The upper and lower parts of Fig. 1 respectively illustrate equilibrium dark adsorption isotherms at 295 K for CHBA onto oxidatively precleaned surfaces of TiO_2(P25) or for the three monochlorophenols in similar conditions [17,19]. Comparison between them establishes the following significant differences; (i) at C_{eq} concentrations ≤ 50 ppm, values of $n^s{}_2$ for the equilibrium extent of adsorption of the hydroxybenzoic acid at each C_{eq} were clearly much larger than for the chlorophenols, as evidenced in particular by attainment of a plateau value equivalent to 100 μmol/gm TiO_2 at $[CHBA]_{eq}$ ~40 ppm, whereas plateau values for the chlorophenols in the same range were almost two-orders-of-magnitude lower; (ii) at higher C_{eq} values the isotherms in both figures evidence an approximately linear increase in $n^s{}_2$ above their respective plateau values, which classical adsorption–desorption models might interpret as evidence for weaker additional adsorption into layers outside the TiO_2/aqueous solution monolayer [20]. Net extent of equilibrium adsorption of the CHBA nevertheless remained at least one order-of-magnitude greater than those of the monochlorophenols across the range studied [17,18].

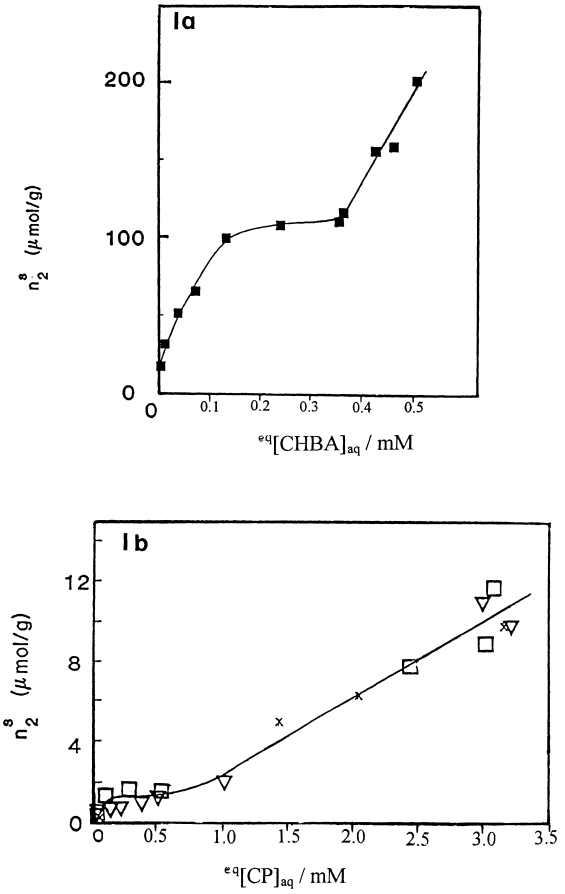

Fig. 1. Equilibrium 'dark' adsorption isotherms data at 295 K ($n^s{}_2$ = amount adsorbed per gram TiO_2) versus C_{eq}, equilibrium aqueous phase concentration, between precalcined TiO_2(P25) and aerated aqueous solutions of: (a) 3-chloro-4-hydroxybenzoic acid (CHBA); and (b) monochlorophenols 2-ClPhOH, □; 3-ClPhOH, X; and 4-ClPhOH, ▽.

3.2. Inverse ratio between initial TiO_2*-PCD rates, $-R^*_i$ of CHBA and ClPhOH

The following assumptions are implicit in the widespread, but not universal, acceptance of some validity in applying to TiO_2*-PCD processes taking place in aqueous TiO_2suspensions, rate equations similar to those developed by Langmuir, Hinshelwood, Hougen and Watson in respect of heterogeneously catalysed reactions at Gas/Solid interfaces [21]: firstly, that reaction events with rate coefficient k_{LH}, involving active species/sites photogenerated at the TiO_2*/aqueous solution interface and some pollutant species adsorbed thereon, constitute the rate- and efficiency-determining process: and secondly, that adsorption–desorption equilibria between pollutant species and the TiO_2 surface are sufficiently fast as to be non-rate-determining. However, Eq. (4) below shows that they may influence the overall rates, -d[*C*]/d*t* of TiO_2*-PCD processes via magnitude of the equilibrium constant, K_{ads}, for adsorption–desorption of pollutant onto the TiO_2 surface.

$$\frac{-\mathrm{d}[C_{eq}]}{\mathrm{d}t} = k_{LH}\frac{K_{ads}C_{eq}}{1 + K_{ads}C_{eq}} \quad (4)$$

On the basis of rate equations of that form, and the much larger value of K_{ads} evidenced for CHBA than for monochlorophenols in Fig. 1, a much larger TiO_2*-PCD rate was to be expected for −d[CHBA]/d*t* than for −d[ClPhOH]/d*t*; – unless compensated for by larger inverse changes in the relative magnitudes of k_{LH} in those two classes of pollutant. Evidence for operation of some such inverse change, causing the apparent k_{LH} for TiO_2*-PC removal of CHBA to be very much *lower* than for the monochlorophenols [22], is contained within Figs. 2 and 3 and discussed in the next paragraphs.

Each data-point on plots within Figs. 2 and 3 orginated from a separate TiO_2*-PC run, during which several samples were syringe-extracted from the continuously-stirred suspension after selected durations of illumination. HPLC analysis of filtrate from the extracted samples yielded values for $[CHBA]_{aq}$ or $[ClPhOH]_{aq}$ remaining after each duration, which were plotted versus illumination time. Initial slopes determined from such plots, termed $-R_i$*, were in turn represented graphically versus initial C_{eq} values to obtain the profiles shown in Figs. 2 and 3. It was hoped that $-R_i$* values evaluated this way, whilst TiO_2*-induced decreases from C_{eq} were ≤10%, would minimise adsorption or kinetic interferences from photoinduced intermediates or products. Comparisons made between $-R_i$* values for CHBA in Fig. 2 and $-R_i$* values in Fig. 3 for ClPhOH, obtained at equivalent C_{eq} values and under identical photon flux, reveal that in almost all situations $-R_i$* for the poorly-adsorbing ClPhOH was substantially higher than $-R_i$* for the well-adsorbing CHBA. Inverse changes in the apparent k_{LH} rate coefficients, sufficient to overcome the greater adsorption of CHBA, could be inferred from such comparison. One

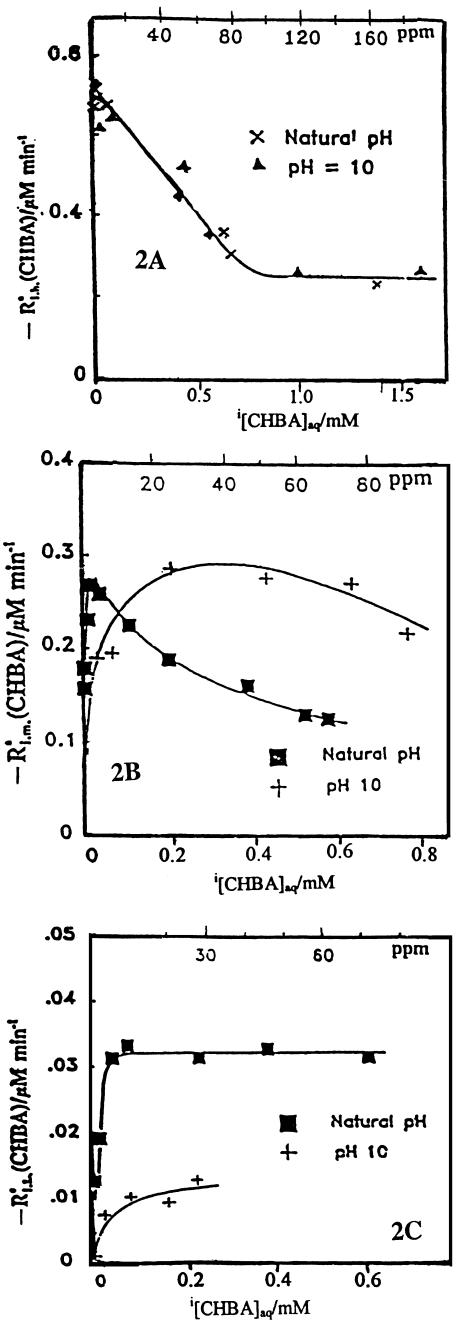

Fig. 2. Plots of initial rates, $-R^{*}_{i}$(CHBA), for TiO_2*-induced decrease from dark pre-equilibrated aqueous-phase concentrations of CHBA, under 'high' flux of 365 nm photons (A); 'moderate' flux (B) and 'low' flux (C) for aerated TiO_2 suspensions, having natural (unadjusted) pH, or with pH adjusted to 10 by $(NaOH)_{aq}$.

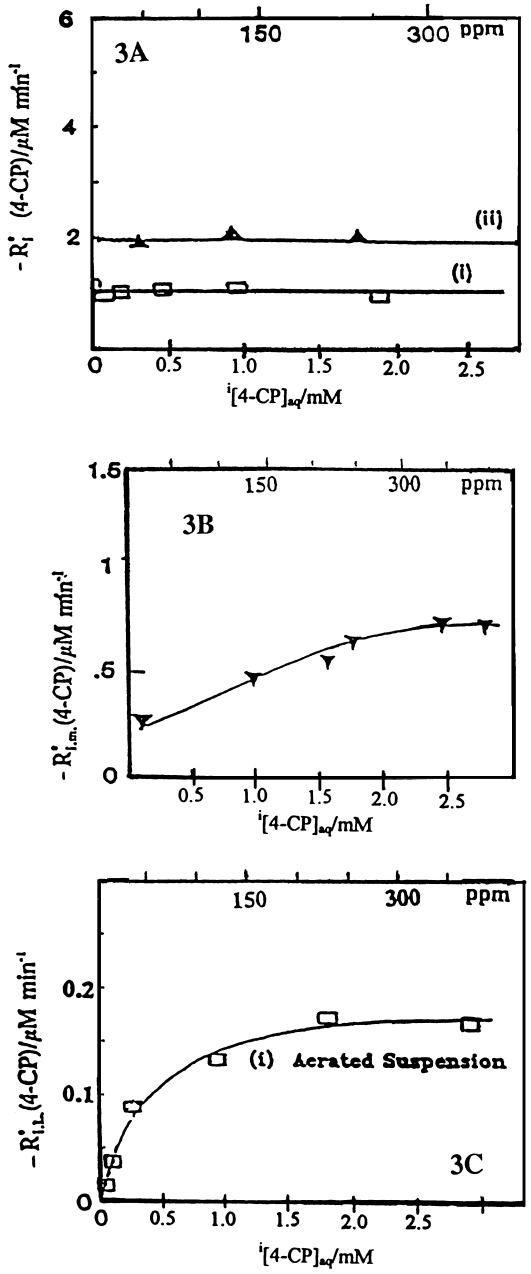

Fig. 3. Plots of initial rates, $-R_{i}^{*}$(4-CP), for TiO_2*-induced decrease from dark pre-equilibrated aqueous phase concentrations of 4-ClPhOH under 'high' flux of 365 nm photons (A), 'moderate' flux (B) and 'low' flux (C). All data for aerated TiO_2 suspensions at natural pH, except plot (ii) in (A) which relate to preoxygenated suspensions.

such process previously proposed [23] is a capability of CHBA species chemisorbed onto TiO_2 to serve as locations capable of enhancing the efficiency of $(e^- + h^+)$ recombination events relative to that at TiO_2/aqueous solution interfaces onto which such chemisorption did not occur.

Another unexpected difference between the $-R_i^*$ versus C_{eq} profiles for CHBA in Fig. 2 and ClPhOH in Fig. 3 was the occurrence of regions of *negative-order* dependence upon C_{eq} for the former, but not for the latter. However, it was only under highest flux used, 2×10^{18} photons min^{-1}, that negative-order dependence of $-R_i^*$(CHBA) upon C_{eq} operated between 100 ppm and the lowest C_{eq} values, (cf. Fig. 2a). Under moderate flux, positive-order was briefly evidenced at C_{eq} up to 5 ppm before a changeover to negative-order at 5–80 ppm (Fig. 2b). Under the lowest flux used, negative-order was not observed. A not-uncommon cause for onset of negative-order behaviour in heterogeneously catalysed reactions is blockage of active sites by some strongly adsorbed product or by-product. Blockage of TiO_2^*-active sites by *photogenerated* product from TiO_2^*-PCD of adsorbed CHBA seemed a somewhat analagous possible cause for the negative-order in Fig. 2a and b, especially since no such blockage was evidenced under low photon flux.

The fact that even under highest photon flux the pre-100 ppm negative-order dependence of $-R_i^*$ upon C_{eq} was succeeded at $C \geq 100$ ppm by a region of zero-order dependence indicated that not all routes to TiO_2^*-photoinitiated removal of CHBA were susceptible to such blockage by photogenerated product. On the other hand zero-order dependence predominated the profile for variation of $-R_i^*$ of poorly adsorbing ClPhOH upon C_{eq} in high flux conditions (cf. Fig. 3a), with no region of negative-order. Furthermore, that rate was ca. five-fold greater than eventually attained by CHBA in its zero-order dependent range. Our earlier hypotheses [23] in explanation of the latter qualitative differences were: (a) that in the case of poorly adsorbing ClPhOH, the *predominant* fate of photogenerated h^+/S_h entities at the illuminated TiO_2^*/solution interface (cf. Scheme 1) was their reaction with OH^- or H_2O to yield OH radicals; and (b) that the latter were capable of diffusing outward into near-surface layers where their reaction with non-adsorbed ClPhOH was assured. The latter hypothesis is now disfavoured by more recent results from experiments of Meisel and Serpone [24] and Minero et al [25] indicating that active species (including $OH_{(s)}$) formed upon irradiation do not migrate in solution. On the other hand, organic species may/may-not migrate to the catalyst surface. It became desirable, therefore, to consider whether contributory factors to the strong differences between kinetic behaviour of the well-adsorbing CHBA and poorly-adsorbing ClPhOH could be differences: (I) in migration of the substrates to photoactive sites; and/or (II) between surface densities of $OH_{(s)}^-$, capable of $OH^-{}_{(s)} + h^+ \rightarrow OH_{(s)}$, at microinterfaces between TiO_2 and $[ClPhOH]_{aq}$ or $[CHBA]_{aq}$.

(I): Light-scattering measurements upon aqueous suspensions of TiO_2(P25) point to the existence of 1–5 μm sized aggregates of the 30 nm sized primary particles [26,27]. Relative difficulties for in-diffusion of weakly-adsorbed and strongly-adsorbed pollutant species from bulk solution inward towards surface sites on TiO_2 particles deep within the aggregates, thus becomes another possible source of difference between strongly-chemisorbing hydroxybenzoic acids and poorly-adsorbing monochlorophenols. Slow outward diffusion, operating in converse manner upon strongly adsorbed photoproduct, may also become a rate-limiting process through lengthening the time required for vacating active TiO_2^* sites upon particles deep within the aggregates. Recently, Bouchy et al. have concluded from their detailed studies of time profiles for approach to equilibrium dark-adsorption in TiO_2 suspensions, that mass transport can indeed be relatively slow through interparticle spaces within such TiO_2 aggregates e.g. with diffusion coefficients comparable to liquid diffusion in zeolites [27]. In the light of those findings, possible influences of such internal mass transport limitation upon efficiency of TiO_2^*-PCD merit serious consideration, especially in respect of the contrast between strongly negative-order of $-R_i^*$ versus $[CHBA]_{eq}$ @ 10–100 ppm (cf. plot A of Fig. 2) and zero-order dependence for $-R_i^*$ versus $[4\text{-CP}]_{eq}$ across the same range (cf. plot A of Fig. 3). Bearing in mind the low extent of adsorption of 4-CP onto TiO_2 relative to the much more extensive dark adsorption of CHBA across the 10–100 ppm concentration range (cf. Fig. 1a), the occurrence of a pronounced negative-order effect only for TiO_2^*-PCD of CHBA might be rationalised as follows: an *impeding*

effect of strongly adsorbed CHBA upon the internal mass transfer processes required to effect removal of well adsorbed photoproduct from within the aggregate out to the bulk solution, and conversely an impeding effect of strongly adsorbed photoproduct upon in-diffusion of adsorbing CHBA species from bulk solution via interparticle spaces to vacated TiO_2 sites within the aggregates.

(II): Dissatisfaction with the somewhat indirect nature of the solution-based evidence leading to the above-noted rationalizations of differing behaviours of CHBA and 4-CP at C_{eq} values in the range 10–100 ppm, caused us to turn to measurements by DRIFTS in efforts to gain *direct* insights into the extent/nature of adsorption of hydroxybenzoic acids or phenols onto TiO_2(P25) from aqueous solution with concentrations in that range. Literature results concerning such points had come from the research of Tunesi and Anderson [28] and of Martin et al. [29] who respectively reported results from in-situ Cylindrical Internal Reflection (CIR) and Attenuated Total Reflectance (ATR) FTIR techniques to obtain insights into the species present at actual Aqueous solution//TiO_2 interfaces. Both investigations used TiO_2 coated as a thin layer onto the external surfaces of a zinc selenide cylinder or trapezoid surrounded by aqueous solution containing the adsorbate of interest. Particularly strong characteristic IR absorbances originating from pollutant species present at the TiO_2/aqueous solution interfaces were reported for 2-hydroxybenzoic acid (salicylic acid) [28] and for 4-chloro catechol [ClCT] from dilute aqueous solutions [29]. These were attributed to probe molecules strongly chemisorbed onto hydroxylated surface Ti^{4+} sites in chelate-like fashions, denoted as bidentate-mononuclear or bidentate-binuclear (cf. Fig. 4a and b). Schematic representations of site-specific chemisorption processes proposed to result from chelation of the catechol species onto TiO_2 are reproduced in Fig. 4A, from which it may be noted that, for each ClCT complexed to the surface in bidentate-binuclear fashion, two hydroxide ions previously present upon TiO_2 are displaced. Chelate-like chemisorption of 2-hydroxybenzoic acid in mononuclear-bidentate manner onto single four-coordinate Ti^{4+} cations upon anatase had earlier been proposed by Tunesi and Anderson [28].

The primary objective of our exploratory DRIFTS measurements was to discover whether insights similar to those just summarised from CIR and ATR-FTIR measurements [28,29] might be obtained by applying DRIFTS measurements to TiO_2(P25) samples onto which salicylic acid or catechol had been dark-adsorbed in conditions closely similar to those employed in our determinations of adsorption isotherms.

The first stage in our procedures towards obtaining DRIFTS spectra of salicylic acid or catechol strongly adsorbed onto/into TiO_2 particles/aggregates involved overnight dark-equilibration between samples of precalcined TiO_2 powder and aqueous solutions with original concentrations 3–100 ppm. Following filtration through a 0.2 μm membrane, the TiO_2 collected thereon was freeze-dried overnight, before mounting the fully dried powder in the diffuse reflectance accessory and obtaining a DRIFTS spectrum therefrom in standardised conditions. A fortuitous outcome of the freeze-drying work-up was the very fluffy nature of the resultant TiO_2, which respresented a condition particularly suited for diffuse reflectance-based detection of adsorbates retained on the TiO_2 particles. Fig. 5 illustrates a DRIFTS spectra thus obtained from dark-equilibration of TiO_2 with a 30 ppm solution of catechol (after subtracting out a reference DRIFTS spectrum measured in identical conditions upon TiO_2 dark-equilibrated with pure H_2O). A satisfactory match existed between the two principal features evident in our DRIFTS spectra at 1486 cm^{-1} and 1261 cm^{-1} and features at 1484 and 1268 cm^{-1} in the IR-data reported by Martin et al [29] who assigned theirs respectively to C=C normal modes and C–O vibrations in the doubly-deprotonated anion produced from ClCT following its chelation to the surface in the manner of Fig. 4A. Making due allowance for presence of the chloride substituent in their ClCP [29], there is satisfactory correspondence between our DRIFTS and their ATR measurements. Such correspondence may even extend to include a small but highly reproducible feature at 1328.7 cm^{-1} clearly evident in our DRIFTS spectra from TiO_2 dark-equilibrated with $[CT]_{aq}$ = 30, 10 or 3 ppm and a small feature just detectable in their published ATR-FTIR from ClCT/TiO_2 at ~1320 cm^{-1}.

Fig. 5b illustrates the more complex pattern of IR features observed by our DRIFTS measurements

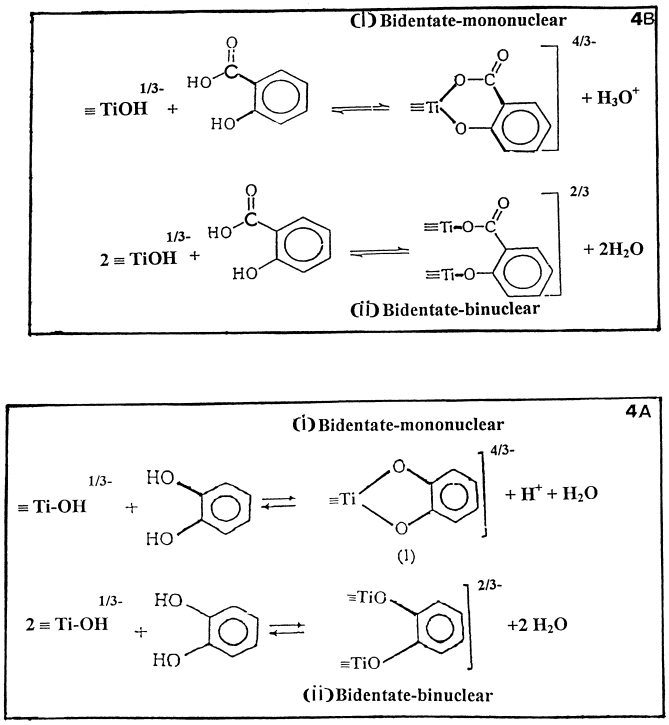

Fig. 4. Schematic representations (adapted from [28,29]) of catechol species from aqueous solution onto hydroxylated TiO_2 (anatase) surface via mononuclear-bidentate-type bonding, A(i); or binuclear-bidentate-type bonding, A(ii); and in B(i) and B(ii) for 2-hydroxybenzoic acid (salicyclic acid).

upon TiO_2 dark pre-equilibrated overnight with a 10 ppm aqueous solution of 2-hydroxybenzoic acid, followed by filtration and freeze-drying. The following pairwise listing (DRIFTS versus CIR) of values for peak positions attributable to adsorbate in the two methods shows adequate correspondence to support a conclusion that the indicated features originated in each case from closely similar salicylate anions chelated to surface Ti^{4+} cations: 1570 versus 1575 or 1538 cm^{-1}, consistent with COO^- stretches; 1450 versus 1457 cm^{-1}, consistent with C–O stretch; and 1399/1367 doublet versus 1386/1367 doublet from coupling between COO^- and C–O bonding. Further work is needed, however, to identify origins of other peaks in DRIFTS spectrum (Fig. 5b).

Thus, relative to IR features reported in the literature on the basis of CIR/ATR-FTIR measurements upon chemisorbed species present at actual (salicylic acid)$_{aq}$/TiO_2 or (ClCT)$_{aq}$/TiO_2 interfaces [28,29], rather similar features were detected by our DRIFTS measurements upon 'dry' (salicyclic acid)$_{ads}$/TiO_2 and 'dry' (catechol)$_{ads}$/TiO_2 samples obtained by freeze-drying TiO_2(P25) powder samples separated from the corresponding dark pre-equilibrated suspensions having initial concentrations as low as 3 ppm. Initially this occasioned some surprise, in view of measures used to control ionic-strength in the ATR-FTIR measurements [29], versus their complete absence from our procedures leading to the DRIFTS spectra. However, if strength of the chelation-type bonds between four-coordinated Ti^{4+} cations and chemisorbed salicylate or ClCT ions were such as to predominate over all other surface interactions, the similarities in FTIR spectra from the two techniques could be understood. Furthermore, the close similarity maintained in our studies between dark-adsorption pretreatments prior to DRIFTS measurements thereon, or measurements of initial rates R^*_i of TiO_2*-PCD thereon, allows the following important inference to be drawn: namely, that the number of surface

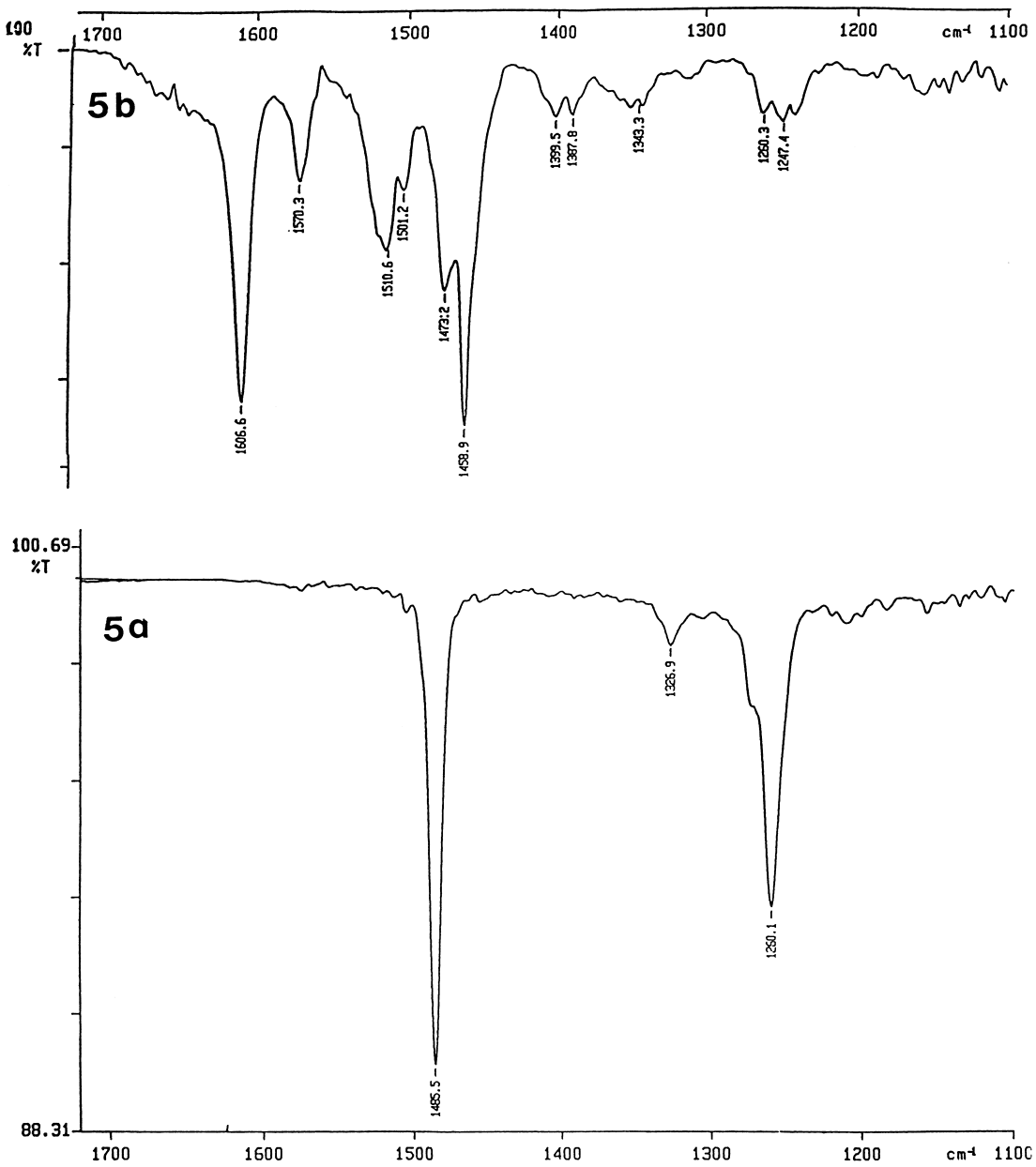

Fig. 5. (a) DRIFTS spectrum from precalcined TiO_2(P25), after dark pre-equilibration with aqueous solution containing 30 ppm catechol, recovery by filtration, and overnight freeze-drying. (b) DRIFTS spectrum from precalcinced TiO_2(P25), after dark pre-equilibrated with aqueous solution containing 10 ppm 2-hydroxybenzoic acid, recovery by filtration and overnight freeze-drying.

hydroxyls remaining upon TiO_2 pre-equilibrated with an adsorbate capable of chelating the surface in ways analagous to those illustrated in Fig. 4 can be substantially diminished relative to those remaining upon TiO_2 pre-equilibrated with weakly adsorbing species which do not chelate surface titanium ions in the manner of Fig. 4. The negative-order behaviour evidence in Fig. 2A for R_i^* of the well-adsorbing CHBA may, in part, originate from such an effect, since decreased availability of surface hydroxyls to capture photogen-

erated holes would diminish the availability of surface OH radicals for oxidation attack upon organics. Such an effect would appear to be the converse of a recent suggestion by Nosaka et al. [30] to the effect 'that the larger the amount of surface OH groups, the more likely the oxidation via surface-trapped holes'.

Also of interest in respect of limitations/capabilities of DRIFTS measurements upon Adsorbate/TiO_2 samples obtained after freeze-drying procedures were preliminary assessments of (a) the lowest detectable coverage of the freeze-dried TiO_2 surface by salicylate or catechol species held thereon in a site-specific manner, as implied by the sharp IR features in Fig. 5a and b; and (b) whether or not the procedures might point to the development of additional types of adsorbed species at the higher extents of surface coverage anticipated from dark pre-equilibration with $[SA]_{aq}$ or $[CT]_{aq} \gg 10$ ppm. Valuable information concerning those points at 'wet' interfaces had been deduced by Martin et al. from their detailed analyses of ATR-FTIR spectra of 4-chlorocatechol [29]. Since our DRIFTS measurements TiO_2 freeze-dried after dark pre-equilibration with very dilute, 3 ppm aqueous solutions of CT or SA reproduced the IR features in Fig. 5a and b, except for ca. five-fold decrease in peak intensities, it could be concluded: (i) that sites indistinguishable from those occupied from 10 ppm solutions were likewise involved in site-specific chemisorption at 3 ppm; and (ii) that fractional coverage equivalent to one twentieth of the total surface area of the dark pre-equilibrated TiO_2 remained detectable. On the other hand, DRIFTS spectra from TiO_2 dark pre-equilibrated with solutions having 30 ppm or 100 ppm of catechol or salicylic acid did not yield proportionate increases in intensities of the previously sharp IR features. Instead significant broadening and slight shifts in band maxima, occurred as confirmed by DRIFTS 'difference-spectra' between samples exposed to 30 ppm and 100 ppm solutions. Heterogeneity of the TiO_2 surface is thus indicated in respect of chemisorption of salicylate ions or catechol from aqueous solutions in the 30–100 ppm range. Further work will be needed to ascertain whether such heterogeneity of the TiO_2(P25) might adequately be accounted for on the basis of site-specific chemisorptions onto *two* such distinguishable sites [28,29], or require consideration of a wider range of chemisorption sites.

4. Conclusions

As an antidote to the preoccupation with two-parameter, Langmuir-Hinshelwood-type mechanisms and rate expressions in much of the literature concerning TiO_2^*-PCD of aqueous-phase organic pollutants, the foregoing text and results stress the need for due cognisance to be taken of the intrinsically multivariable character of the TiO_2^*-PCD process. The strong influences of nature/strength of pollutant adsorption onto TiO_2 in respect of such interdependences is evidenced by the following:

1. Chemisorbed versus physisorbed nature of pollutant adsorption and, in the case of micron-sized TiO_2-aggregates in aqueous suspensions, large consequential differences in extent of internal-mass-transport limitations through interparticle spaces between 30 nm TiO_2(P25) particles within the micron-sized aggregates.
2. In respect of the nature of primary conversions experienced by TiO_2^*-photogenerated charge-carriers at monolayer TiO_2^*/aqueous solution micro-interfaces, these too can be more significantly affected by chemisorbed species e.g. through decreases in $[OH^-]_s$.
3. Under high flux of near-UV photons, very different order-of-reaction is observed in kinetics of post-primary redox processes during TiO_2^*-PCD over micron-sized TiO_2 aggregates pre-equilibrated respectively with strongly-adsorbing or weakly-adsorbing pollutant from 50 ± 40 ppm solutions. These differences can be rationalised when conclusions (1) and (2) above are taken into account.

Acknowledgements

Those aspects of the reported work which were carried out at University College Cork benefited greatly from support received under EC contracts EV4V0068 and STEP 0106-C.

References

[1] D. Bahnemann, J. Cunningham, M.A. Fox, E. Pelizzetti, P. Pichat and N. Serpone, in: G.R. Helz, R.G. Zepp, D.G. Crosby

(Eds.), Aquatic and Surface Photochemistry, chap. 1, Lewis Publishers, Boca Raton, Florida, 1994, pp. 261–316.
[2] L. Amalric, C. Guillard, P. Pichat, Res. Chem. Intermed. 20 (1994) 579.
[3] H. Gerischer, A. Heller, J. Phys. Chem. 95 (1991) 5261.
[4] S. Tunesi, M. Anderson, J. Phys. Chem. 95 (1991) 3399.
[5] C. Richard, J. Photochem. Photobiol. A. Chem. 72 (1993) 179.
[6] C. Minero, E. Pelizzetti, S. Malato, J. Blanco, Solar Energy 56 (1996) 411 and 421.
[7] C. Minero, E. Pelizzetti, S. Malato, J. Blanco, Chemosphere 26 (1993) 2103.
[8] E. Pelizzetti, C. Minero, V. Carlin, M. Vincenti, E. Pramauro, Chemosphere 24 (1992) 2103.
[9] C. Minero, E. Pelizzetti, S. Malato, J. Blanco, Solar Energy 56 (1996) 421.
[10] C. Minero, Solar Energy Materials and Solar Cells 38 (1995) 421.
[11] P. Calza, C. Minero, E. Pelizzetti, Environ. Sci. Technol. 31 (1997) 2198.
[12] P. Calza, C. Minero, E. Pelizzetti, J. Chem. Soc. Faraday Trans. 93 (1997) 3765.
[13] K.A. Gray, U. Stafford, Res. Chem. Intern. 20 (1994) 835.
[14] K. Vinodgopal, S. Hotchandani, P. Kamat, J. Phys. Chem. 97 (l993) 9040.
[15] H. Tada, M. Tanaka, Langmuir 13 (1997) 360.
[16] M. Graetzel, Energy Resources Through Photochemistry and Catalysis, Academic Press, New York, 1983.
[17] J. Cunningham, G. Al-Sayyed, J. Chem. Soc. Faraday Trans. 86 (1990) 3935.
[18] J. Cunningham, P. Sedlak, J. Photochem. Photobiol. A. Chem. 77 (1994) 255.
[19] J. Cunningham, G. Al-Sayyed, S. Srijaranai, in: G.R. Helz, R.G. Zepp, D.G. Crosby (Eds.), Aquatic and Surface Photochemistry, chap. 22, Lewis Publishers, Boca Raton, Florida, 1994, p. 317.
[20] R.P. Hansen, R.P. Craig, J. Phys. Chem. 58 (1954) 212.
[21] M. Boudart, G. Djega-Mariadassou, Kinetics of Heterogeneous Catalytic Reactions, Princeton University Press, Princeton, NJ, p. 92 and 106.
[22] J. Cunningham, P. Sedlak, Catal. Today 29 (1996) 309.
[23] J. Cunningham, P. Sedlak, in: D.F. Ollis, H. Al-Ekabi (Eds.), Photocatalytic Purification and Treatment of Air and Water, Elsevier, Amsterdam, 1993, pp. 67–81.
[24] D. Meisel, N. Serpone, J. Phys. Chem. 95 (1991) 199.
[25] C. Minero, F. Catozzo, E. Pelizzetti, Langmuir 8 (1992) 481.
[26] R.I. Bickley, T. Gonzalez-Carreno, J.S. Lees, L. Palmisano, R.J.D. Tilley, J. Solid State Chem. 92 (1991) 178.
[27] H.Y. Chen, O. Zahraa, M. Bouchy, F. Thomas, J.Y. Bottero, J. Photochem. Photobiol. A. Chem. 85 (1995) 179.
[28] S. Tunesi, M. Anderson, Langmuir 8 (1992) 487.
[29] S. Martin, J.M. Kesselman, D.S. Park, N.S. Lewis, M.F. Hoffmann, Environ. Sci. Technol. 30 (1996) 2535.
[30] Y. Nosaka, N. Kishimoto, F. Nishino, J. Phys. Chem. 102 (1998) 10279.